CHEMICAL PHYSICS

Cavity-enabled enhancement of ultrafast intramolecular vibrational redistribution over pseudorotation

Teng-Teng Chen[1]†, Matthew Du[1]†, Zimo Yang[2]†, Joel Yuen-Zhou[1]*, Wei Xiong[1,2,3]*

Vibrational strong coupling (VSC) between molecular vibrations and microcavity photons yields a few polaritons (light-matter modes) and many dark modes (with negligible photonic character). Although VSC is reported to alter thermally activated chemical reactions, its mechanisms remain opaque. To elucidate this problem, we followed ultrafast dynamics of a simple unimolecular vibrational energy exchange in iron pentacarbonyl [Fe(CO)$_5$] under VSC, which showed two competing channels: pseudorotation and intramolecular vibrational-energy redistribution (IVR). We found that under polariton excitation, energy exchange was overall accelerated, with IVR becoming faster and pseudorotation being slowed down. However, dark-mode excitation revealed unchanged dynamics compared with those outside of the cavity, with pseudorotation dominating. Thus, despite controversies around thermally activated VSC modified chemistry, our work shows that VSC can indeed alter chemistry through a nonequilibrium preparation of polaritons.

Vibrational strong coupling (VSC) gives rise to delocalized superpositions of molecular vibrations and electromagnetic modes (cavity modes), known as molecular vibrational polaritons (1, 2). Recently, VSC has become a promising method for manipulating chemical reactions in condensed phases (3–5). Extensive experimental evidence has shown that without photoexcitation, reaction rates can be either accelerated or decelerated by VSC and reaction selectivity can even be altered (3–5). Although much effort has been devoted to providing a sound explanation for VSC-modified chemistry, consensus between theory and experiments is still missing (6–11). Though it is clear that polaritons are different from bare molecular states, and thereby have the potential to modify chemistry, dark modes, which greatly outnumber polaritons, have the same excitation energies as the uncoupled vibrational modes (12). Hence, some theoretical work predicts that reactivity in the collective VSC regime is similar to that outside an optical cavity (6, 8, 9, 13), which is consistent with a few recent experimental results that show no modification of reactions from VSC (10, 14). Resolution of the discrepancies is hindered by the following factors: Most reactions studied so far are quite complex, that is, involve multiple steps or are diffusion limited; and reactive events involving dark modes and polaritons simultaneously are probed together (3–5). To delineate the effect of VSC, it is there-fore critical to study elementary reactions and use a technique that can differentiate the contributions from polaritons and dark modes.

Here, we used ultrafast two-dimensional infrared (2D IR) spectroscopy to follow how the polaritons and dark modes evolve in both pseudorotation and intramolecular vibrational-energy redistribution (IVR) of Fe(CO)$_5$ (15). We did so in a state-resolved manner, thereby meeting the desired criteria listed earlier. Fe(CO)$_5$ features two IR-active vibrational bands, a doubly degenerate e′ mode at 1999 cm^{-1} that involves three equatorial CO groups, and an a$_2$″ mode at 2022 cm^{-1} that involves the axial CO groups (fig. S1). Harris and co-workers applied 2D IR spectroscopy and showed that Fe(CO)$_5$ can rearrange from its D$_{3h}$ equilibrium geometry to a C$_{4v}$ transition state and back to D$_{3h}$, during which the equatorial and axial CO ligands interconvert, leading to vibrational energy exchange between the a$_2$″ and e′ modes (16). This process, referred to as Berry's pseudorotation, is a single barrier crossing and thus represents the essence of elementary reactions, although the product is indistinguishable from the reactant (17). Given that Berry's pseudorotation competes with IVR between a$_2$″ and e′ modes whose transition dipoles are perpendicular to each other (Fig. 1A, top), Fe(CO)$_5$ is an ideal testbed to understand how VSC affects single barrier-crossing events and the branching ratio between various dynamical processes.

Using 2D IR spectroscopy, we found that when polaritons were pumped, they could accelerate the overall 2D IR cross-peak dynamics, and more notably, the excited polaritons make IVR faster than pseudorotation (bottom of Fig. 1A). By contrast, the dynamics triggered by exciting the dark reservoir modes were similar to the dynamics of molecules outside the cavity. Thus, the fundamental concept of VSC-modified chemistry—that polaritons can change reactions—holds. However, because dark modes are statistically dominant, the overall influence of VSC on the dynamics of Fe(CO)$_5$, when measured without differentiating polariton and dark modes (e.g., without optical pumping at room temperature), should be negligible.

The VSC condition was achieved by placing a solution of Fe(CO)$_5$ in n-dodecane into a Fabry-Pérot microcavity. Unless specifically mentioned, we set the Fe(CO)$_5$ concentration to ~180 mM and the cavity longitudinal thickness to ~12.5 μm. The e′ and a$_2$″ vibrational modes of Fe(CO)$_5$ strongly couple to a fifth-order cavity mode. The IR spectrum (Fig. 1B) shows the transitions of upper, middle, and lower polaritons (UP, MP, and LP) at a resonant frequency (ω) of ω$_{UP}$ = 2045 cm^{-1}, ω$_{MP}$ = 2014 cm^{-1}, and ω$_{LP}$ = 1976 cm^{-1}, respectively. By fitting to a coupled oscillator model [see supplementary materials (SM) section 2.1], we determined that the cavity mode is 2013 cm^{-1} and it interacts with the e′ and a$_2$″ modes with amplitudes g$_{cav-e′}$ = 26 cm^{-1} and g$_{cav-a2″}$ = 19 cm^{-1}, respectively. Because the full widths at half maximum of the e′ and a$_2$″ modes are 8 and 5 cm^{-1}, respectively, and that of the cavity mode is 11 cm^{-1}, the samples satisfy the criteria for VSC (18).

We used 2D IR to monitor the cross-peak dynamics both outside and inside the cavity (19–22). Through pseudorotation and IVR, the a$_2$″ and e′ modes can exchange energy. By measuring the dynamics of the [2022, 1986] cross and [2022, 2010] diagonal peaks of the 1→2 transitions (fig. S6) and fitting them to a kinetic model (see SM section 2.3.1), we determined the energy-exchange rate constant k$_{ex}$ to be 0.084 ± 0.002 ps^{-1} at 25°C (Fig. 1D). Here, unless specifically mentioned, all measurements were done under magic angle conditions to remove contributions from rotational dynamics.

Similarly, for Fe(CO)$_5$ under VSC (Fig. 1C), we followed the dynamics of the [ω$_{UP}$, ω$_{MP}$] (red box in Fig. 1C) and [ω$_{UP}$, ω$_{LP}$] (blue box in Fig. 1C) peaks of the 2D IR spectrum (or the corresponding narrowband pump probe spectra; see SM section 1.3 for details). Here, we specifically focused on the dynamics involving pumping the UP to avoid complications of hot (i.e., highly excited) vibrational states when exciting the LP mode (23). The interpretation of these peaks was discussed in our previous work (20). Basically, the polariton transitions at ω$_{MP}$ and ω$_{LP}$ overlap with the 1→2 transition of the a$_2$″ and e′ modes, respectively [this assignment is further confirmed by spectral simulations (SM section 2.6) and input-output theory (SM section 4)]. Upon exciting the UP, when the waiting time was beyond the polariton lifetime, the [ω$_{UP}$, ω$_{MP}$] and [ω$_{UP}$, ω$_{LP}$] peaks corresponded, respectively, to the excited state population of

[1]Department of Chemistry and Biochemistry, University of California, San Diego, La Jolla, CA, USA. [2]Materials Science and Engineering Program, University of California, San Diego, La Jolla, CA, USA. [3]Department of Electrical and Computer Engineering, University of California, San Diego, La Jolla, CA, USA.
*Corresponding author. Email: joelyuen@ucsd.edu (J.Y.-Z.); w2xiong@ucsd.edu (W.X.)
†These authors contributed equally to this work.

the a_2'' and e' modes. Therefore, the dynamics of these peaks reported the energy transfer between the a_2'' and e' modes that was facilitated by pseudorotation and IVR. At a first glance, the dynamics of energy transfer under

VSC (reported by $[\omega_{UP}, \omega_{MP}]$ and $[\omega_{UP}, \omega_{LP}]$ peak dynamics) were a bit faster than those of outside the cavity (reported by the [2022, 2010] diagonal and [2022, 1986] cross-peak dynamics) (Fig. 1D).
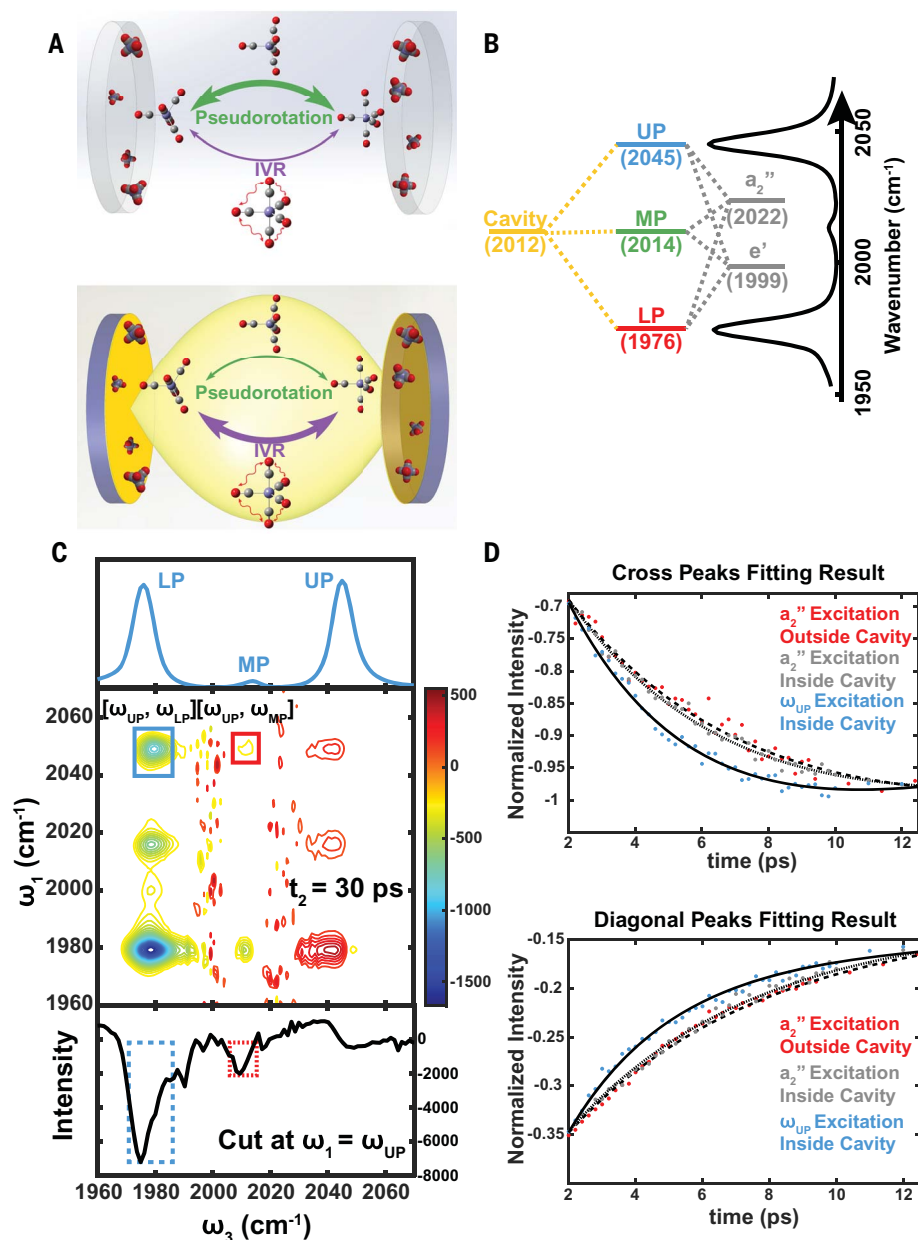
To quantify the energy-exchange dynamics upon pumping the UP, we used the kinetic model shown in Fig. 2A. First, the population of the UP relaxed to both the a_2'' and e' dark modes within the polariton lifetime. Then, the a_2'' and e' dark modes exchanged energy, through pseudorotation and IVR, and at the same time dissipated energy to their environment. The solution of this kinetic model provided a good fit to the $[\omega_{UP}, \omega_{MP}]$ and $[\omega_{UP}, \omega_{LP}]$ dynamics (Fig. 2B). Furthermore, the measured dynamics could be separated into three components: polariton relaxation to dark modes at short times (cavity leakage is implicitly accounted for; see SM section 2.3.2), energy exchange at intermediate times, and vibrational decay at long times. From the fitted
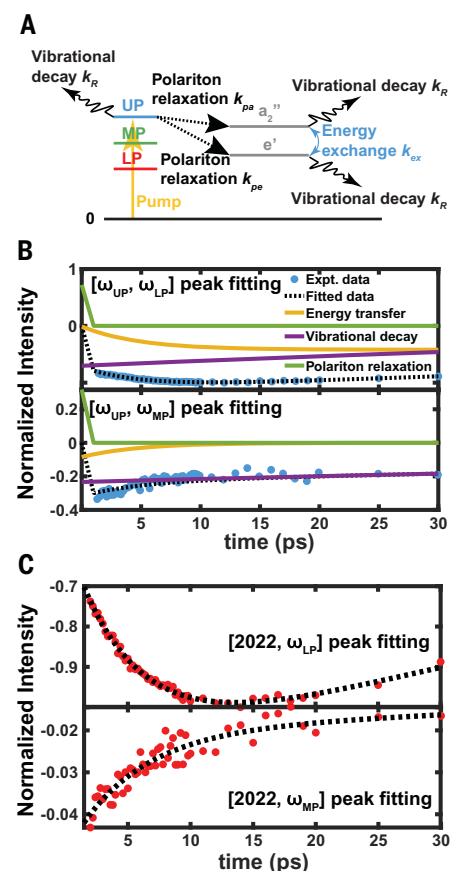

Fig. 1. Influence of VSC on Fe(CO)₅ energy-exchange dynamics. (**A**) Schematic drawing showing that when Fe(CO)₅ is outside of the cavity, pseudorotation is the dominating channel (top); when the molecule is placed in an optical cavity, IVR becomes the dominant energy-exchange process and pseudorotation is suppressed (bottom). (**B**) Strong coupling diagram and IR spectrum of Fe(CO)₅ inside the cavity. (**C**) Normalized 2D IR spectrum using the linear spectrum of strongly coupled Fe(CO)₅ at waiting time (t_2) = 30 ps in dodecane (blue and red boxes represent $[\omega_{UP}, \omega_{LP}]$ and $[\omega_{UP}, \omega_{MP}]$ peaks, respectively), along with the corresponding linear spectrum (top) and normalized narrowband pump probe spectrum at $\omega_1 = \omega_{UP}$ (bottom). (**D**) Experimental dynamics of cross-peaks (top) and diagonal peaks (bottom) for Fe(CO)₅ outside the cavity upon pumping of the a_2'' modes (red dots) and inside the cavity upon pumping of the UP (blue dots) and the a_2'' dark modes (gray dots). The black dashed, dotted, and solid lines are the corresponding fits. Energy is exchanged at a faster rate when pumping the UP, whereas pumping the a_2'' dark modes leads to a rate similar to that outside the cavity.

Fig. 2. Energy-exchange dynamics between a_2'' and e' modes. (**A**) Schematic drawing of the kinetic model for Fe(CO)₅ under VSC. See SM section 2.3.2 for details of the kinetic model. k_{pe} (k_{pa}), the rate constant for the polariton relaxation from UP to the e' (a_2'') modes; k_{ex}, the energy transfer rate constant between the e' and a_2'' modes; k_R, the rate constant for the vibrational decay. (**B**) Experimental data (blue dots) and fits (black dotted lines) including each component for $[\omega_{UP}, \omega_{LP}]$ (top) and $[\omega_{UP}, \omega_{MP}]$ (bottom) peaks. (**C**) Experimental data (red dots) and fits (black dotted lines) for the [2022, ω_{LP}] (top) and [2022, ω_{MP}] (bottom) peaks when the a_2'' dark modes are pumped.

results, k_{ex} under VSC was 0.113 ± 0.009 ps^{-1} at room temperature, 30% faster than that outside the cavity.

Using 2D IR and the same analysis, we found when exciting the a_2'' dark reservoir modes directly, the energy-exchange dynamics had similar trends as those outside the cavity (Fig. 2C) and k_{ex} was 0.090 ± 0.006 ps^{-1}. Clearly, VSC was only modifying the dynamics when the polaritons were pumped, whereas pumping the a_2'' dark reservoir modes caused the system to evolve similarly to the molecules outside the cavity, agreeing with the reservoir's purely molecular character. Similar findings have been predicted by a recent theoretical work (24). The contrast of dynamics between pumping the UP and dark a_2'' modes suggests that the energy-exchange rates depend on the initial populated states.

Although we have shown that VSC leads to faster energy exchange between the a_2'' and e' modes, this acceleration could be due to an enhancement of either pseudorotation or IVR. To qualitatively distinguish between the two processes, we measured the vibrational anisotropy (25) associated with the cross-peaks. IVR involved energy transfer between e' and a_2'' modes that were perpendicular to each other (Fig. 3A), and pseudorotation caused energy exchange between e' and a_2'' modes that were parallel to each other (Fig. 3B). Thus, the anisotropy should start from −0.2 and 0.4 for the former and latter (25, 26), respectively. In general, both processes occurred concurrently, and the initial anisotropy was between these values.

Outside the cavity, the initial value of anisotropy was ~0.06 for exciting the a_2'' modes (Fig. 3C), suggesting that pseudorotation dominated over IVR. However, under VSC, the opposite trend was observed: The anisotropy started at about −0.08 for exciting the UP (Fig. 3D). This contrast indicates that under VSC, IVR dominated over pseudorotation. Not surprisingly, when pumping the a_2'' dark modes under VSC, the anisotropy was ~0.06 (fig. S18), similar to the cavity-free case.

To determine the rate constants of pseudorotation and IVR, a more-detailed kinetic model was developed (see SM section 2.4) (25, 26). The anisotropy can be calculated based on the energy-exchange dynamics simulated from the kinetic model. By fitting the measured anisotropy dynamics to the kinetic model, we determined the rate constants for pseudorotation (k_{ps}) and IVR (k_{IVR}) to be 0.035 ± 0.001 and 0.024 ± 0.001 ps^{-1}, respectively, outside the cavity (Fig. 3C) and 0.022 ± 0.005 and 0.043 ± 0.002 ps^{-1} under VSC (Fig. 3D). The energy-exchange rate is $k_{ex} = k_{ps} + 2*k_{IVR}$ because the pseudorotation adiabatically morphs the a_2'' mode into one of the e' modes but the IVR causes relaxation of a_2'' into both e'' modes (see SM, section 2.4.1e). The former results qualitatively agree with previous work show-

ing that pseudorotation dominated the dynamics outside a cavity (16), except that now we quantified the relative contribution of IVR. The quantitative results agreed with the qualitative analysis above, indicating that VSC shifted the balance between pseudorotation and other energy-exchange channels: Outside the cavity, exciting the a_2'' mode yielded dynamics where pseudorotation dominated over IVR, and under VSC, exciting the UP promoted IVR and suppressed pseudorotation; yet, under VSC, exciting the a_2'' dark modes did not change the dynamics relative to molecules outside the cavity. We note that this

effect is VSC-exclusive, because weak coupling to the cavity did not lead to the modification of the dynamics (see SM section 3.4); further, the acceleration of energy transfer and promotion of IVR through VSC was robust against different solvent environments (see results for 1-octanol, SM section 3.9).

The sharp contrast between the VSC dynamics starting in the UP and a_2'' dark reservoir modes is interesting because, even when the UP was excited, the population relaxed to the dark modes on a much shorter time scale than pseudorotation and IVR. The difference then lies in the relaxation processes available to the
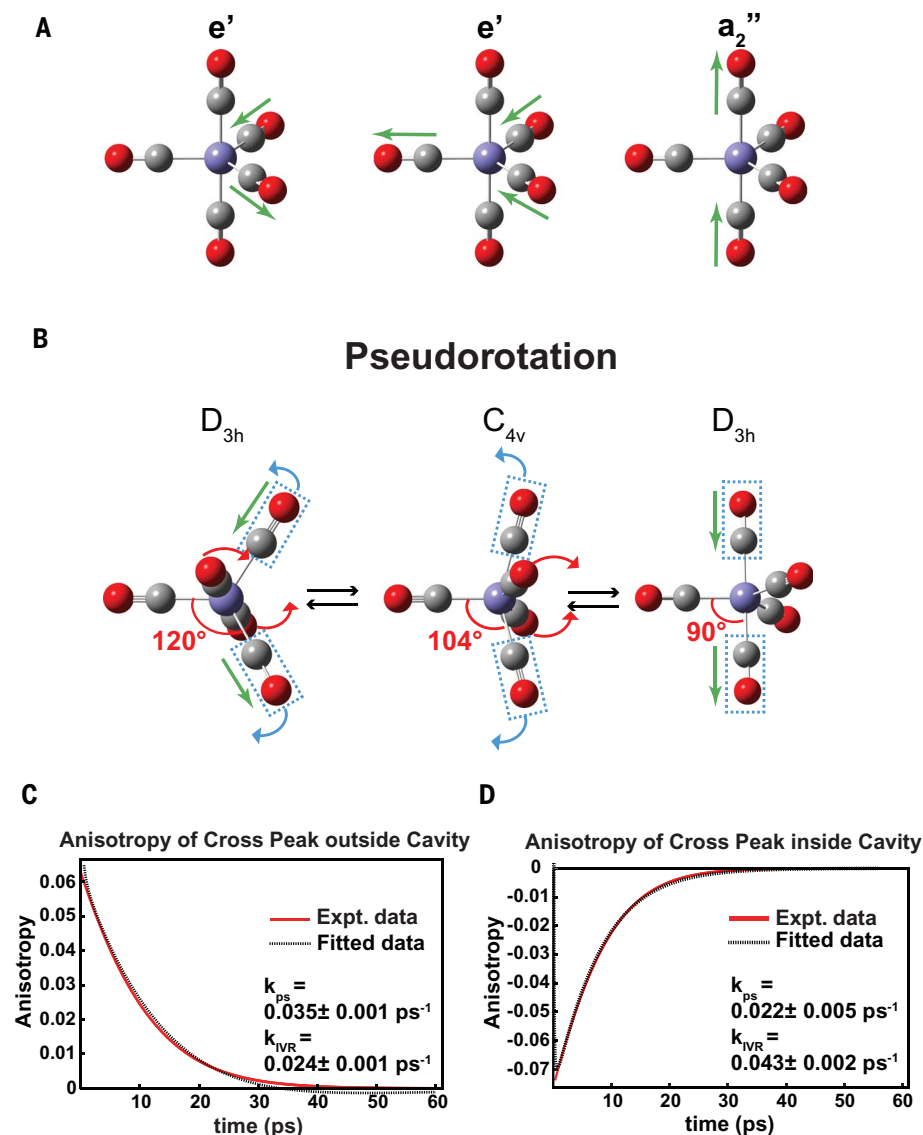

Fig. 3. Cross-peak anisotropy dynamics of IVR and pseudorotation. (**A**) Depiction of the eigenvectors for the a_2'' and doubly degenerate e' vibrational modes of Fe(CO)$_5$. IVR leads to energy transfer between modes that are perpendicular to each other. (**B**) Pseudorotation leads to energy transfer between a_2'' and e' modes that are parallel to each other. (**C** and **D**) Experimental anisotropy (red line) and corresponding fits (black dotted line) for the cross-peak of Fe(CO)$_5$ (C) outside the cavity ([2022, 1986]) and (D) under VSC ([ω_{UP}, ω_{MP}]). Listed are the rate constants, extracted from the fitting, of IVR (k_{IVR}) and pseudorotation (k_{ps}). The rate constants indicate that VSC accelerated IVR and suppressed pseudorotation.

initial states. Several mechanisms could explain the faster IVR upon pumping the UP. For example, the decay from the UP to the a_2'' dark modes was accompanied by the excitation of low-frequency vibrations (i.e., phonons), and some of these phonons could be further excited during the energetically downhill IVR from a_2'' to e' modes. It follows that IVR would be accelerated by the first scattering process, and this enhancement would not occur if the system were initialized in the a_2'' dark modes. A limitation of this hypothesis is that at room temperature, the phonons should have a high occupation number (≈ 10), which should not substantially change when the UP relax to dark modes (through one- or few-phonon excitation). Another possibility is that the VSC-induced speedup in the dynamics reflects a polariton-induced intermolecular vibrational energy transfer. In this case, though, the observed anisotropy dynamics should practically be zero, or have a fast decay (20), instead of starting from a negative value, owing to the lack of orientational correlation between donor and acceptor molecules. Conversely, the mild suppression of pseudorotation is surprising, because it is conventionally thought that these high-frequency vibrational modes do not drive the reaction. However, the coexistence of IVR enhancement and pseudorotation suppression suggests otherwise. By quickly going through IVR, molecules may lose their driving force for pseudorotation, leading to the pseudorotation slowdown. It is also possible that the pseudorotation motion is hindered by the phonons that are excited by the transition from the UP to the dark modes. The temperature-dependent measurements further showed that VSC shifts the thermodynamic parameters of activation in the same direction (see SM section 2.4), which has also been observed—and rather consistently—in reports of reaction kinetics altered by VSC (27). This correspondence supports that the insights obtained here should be relevant to understanding the previous experiments (28).

By using 2D IR to resolve ultrafast chemical dynamics with specific initial states, we quantified the energy-exchange dynamics in $Fe(CO)_5$ under VSC. We showed that when the UP was excited under VSC, IVR was promoted and pseudorotation was suppressed compared with the bare molecular system. However, pumping the dark reservoir modes under VSC led to little change in the dynamics compared with those outside the cavity. Because the population at thermal equilibrium resides predominantly in the dark modes, the overall influence of VSC on $Fe(CO)_5$ should be negligible without external (e.g., laser) pumping. Yet, the present results show an important insight that unifies the works that report VSC-modified reactions and the ones that report or predict the opposite: Regardless of how reactions behave under thermally activated conditions, the basic concept of VSC-modified chemistry works—populated polaritons can influence chemical dynamics. These findings suggest that the future of VSC-modified thermal chemistry lies in controlling the dark modes, either by reducing the number of dark reservoir modes (29) or even going to the single-molecule regimes (30), for example, through cavity miniaturization or by making dark modes more delocalized through heterogeneity (31, 32).

REFERENCES AND NOTES

1. J. P. Long, B. S. Simpkins, *ACS Photonics* **2**, 130–136 (2015).
2. A. Shalabney et al., *Nat. Commun.* **6**, 5981 (2015).
3. A. Thomas et al., *Angew. Chem. Int. Ed.* **55**, 11462–11466 (2016).
4. A. Thomas et al., *Science* **363**, 615–619 (2019).
5. F. J. Garcia-Vidal, C. Ciuti, T. W. Ebbesen, *Science* **373**, eabd0336 (2021).
6. J. Galego, C. Climent, F. J. Garcia-Vidal, J. Feist, *Phys. Rev. X* **9**, 021057 (2019).
7. T. E. Li, A. Nitzan, J. E. Subotnik, *J. Chem. Phys.* **152**, 234107 (2020).
8. I. Vurgaftman, B. S. Simpkins, A. D. Dunkelberger, J. C. Owrutsky, *J. Phys. Chem. Lett.* **11**, 3557–3562 (2020).
9. M. Du, J. A. Campos-Gonzalez-Angulo, J. Yuen-Zhou, *J. Chem. Phys.* **154**, 084108 (2021).
10. M. V. Imperatore, J. B. Asbury, N. C. Giebink, *J. Chem. Phys.* **154**, 191103 (2021).
11. X. Li, A. Mandal, P. Huo, *Nat. Commun.* **12**, 1315 (2021).
12. J. A. Campos-Gonzalez-Angulo, J. Yuen-Zhou, *J. Chem. Phys.* **156**, 194308 (2022).
13. J. A. Campos-Gonzalez-Angulo, J. Yuen-Zhou, *J. Chem. Phys.* **152**, 161101 (2020).
14. G. D. Wiesehan, W. Xiong, *J. Chem. Phys.* **155**, 241103 (2021).
15. R. S. Berry, *J. Chem. Phys.* **32**, 933–938 (1960).
16. J. F. Cahoon, K. R. Sawyer, J. P. Schlegel, C. B. Harris, *Science* **319**, 1820–1823 (2008).
17. F. H. Westheimer, *Acc. Chem. Res.* **1**, 70–78 (1968).
18. P. Törmä, W. L. Barnes, *Rep. Prog. Phys.* **78**, 013901 (2014).
19. B. Xiang et al., *Proc. Natl. Acad. Sci. U.S.A.* **115**, 4845–4850 (2018).
20. B. Xiang et al., *Science* **368**, 665–667 (2020).
21. B. Xiang, J. Wang, Z. Yang, W. Xiong, *Sci. Adv.* **7**, eabf6397 (2021).
22. B. Xiang, W. Xiong, *J. Chem. Phys.* **155**, 050901 (2021).
23. B. Xiang et al., *J. Phys. Chem. A* **123**, 5918–5927 (2019).
24. D. Wellnitz, G. Pupillo, J. Schachenmayer, *Commun. Phys.* **5**, 120 (2022).
25. R. M. Hochstrasser, *Chem. Phys.* **266**, 273–284 (2001).
26. A. Tokmakoff et al., *J. Chem. Phys.* **102**, 3919–3931 (1995).
27. K. Hirai, J. A. Hutchison, H. Uji-I, *ChemPlusChem* **85**, 1981–1988 (2020).
28. A. D. Dunkelberger, B. S. Simpkins, I. Vurgaftman, J. C. Owrutsky, *Annu. Rev. Phys. Chem.* **73**, 429–451 (2022).
29. T. E. Li, A. Nitzan, J. E. Subotnik, *J. Chem. Phys.* **154**, 094124 (2021).
30. C. C. Schäfer, J. Flick, E. Ronca, P. Narang, A. Rubio, arXiv:2104.12429 [quant-ph] (2021).
31. G. D. Scholes, *Proc. R. Soc. London Ser. A* **476**, 20200278 (2020).
32. M. Du, J. Yuen-Zhou, *Phys. Rev. Lett.* **128**, 096001 (2022).
33. T.-T. Chen, M. Du, Z. Yang, J. Yuen-Zhou, W. Xiong, Cavity-enabled enhancement of ultrafast intramolecular vibrational redistribution over pseudorotation, Zenodo (2022); https://doi.org/10.5281/zenodo.7110883.

SUPPLEMENTARY MATERIALS

science.org/doi/10.1126/science.add0276
Materials and Methods
Supplementary Text
Figs. S1 to S45
Tables S1 to S7
References (34–42)

Cavity-enabled enhancement of ultrafast intramolecular vibrational redistribution over pseudorotation

Teng-Teng Chen, Matthew Du, Zimo Yang, Joel Yuen-Zhou, and Wei Xiong

Spectroscopy for polaritonic chemistry

There is currently considerable interest in understanding the effect of vibrational strong coupling (VSC), a promising route to manipulating chemical dynamics in condensed phases. Previous studies of VSC-modified chemistry used traditional chemical kinetics tools that cannot properly address ultrafast vibrational processes in their natural time scales. Using ultrafast two-dimensional infrared spectroscopy, Chen *et al.* showed that polaritons (delocalized superpositions of vibrations and electromagnetic cavity modes) can switch the rates of two vibrational energy pathways of a metal carbonyl compound under VSC, making intramolecular vibrational redistribution more favorable over pseudorotation (the opposite is true outside of a cavity) (see the Perspective by Chuntonov). The authors also clarified the role of dark modes in VSC, a longtime question that has been heavily debated but had lacked direct experimental evidence. —YS

View the article online
https://www.science.org/doi/10.1126/science.add0276
Permissions
https://www.science.org/help/reprints-and-permissions